

Linear-Quadratic Model Predictive Control for Continuous-time Systems with Time Delays and Piecewise Constant Inputs

Zhanhao Zhang, Anders H.D. Christensen,
Jan Lorenz Svensen, Steen Hørsholt, John Bagterp Jørgensen

*Department of Applied Mathematics and Computer Science, Technical
University of Denmark, DK-2800 Kgs. Lyngby, Denmark (e-mail:
jbjo@dtu.dk).*

Abstract:

Exact discretization of continuous linear time-delay systems with quadratic objective functions, under piecewise constant manipulated variables, is used to design and implement a novel linear model predictive controller, termed the continuous-time linear-quadratic model predictive controller (CT-LMPC). The key novelty in the paper is the exact numerical discretization of CT time-delay linear-quadratic systems. The control model of the CT-LMPC is parameterized using transfer functions with delays. We formulate linear-quadratic optimal control problems (LQ-OCPs) with time delays for the CT-LMPC and derive their discretization under the assumption of piecewise constant inputs. Time-delay systems are ubiquitous in process industries, such as the cement industry, where conveyor belts introduce delays, making continuous-time modeling advantageous. We illustrate the CT-LMPC with both SISO and MIMO examples inspired by the cement industry. The results demonstrate that, for fixed parameters, the CT-LMPC outperforms the conventional discrete-time LMPC as the sampling time increases.

Keywords: Linear-quadratic optimal control problems (LQ-OCPs), linear model predictive control (LMPC), Time delay systems, Numerical discretization

1. INTRODUCTION

Consider the following continuous-time (CT) linear-quadratic optimal control problem (LQ-OCP) with piecewise constant inputs (Zhang et al., 2024a,b)

$$\min \phi = \int_{t_0}^{t_0+T} l_c(\tilde{z}(t)) dt \quad (1a)$$

$$s.t. \quad x(t_0) = \hat{x}_0, \quad (1b)$$

$$u(t) = u_k, \quad t_k \leq t < t_{k+1}, \quad k \in \mathcal{N}, \quad (1c)$$

$$\dot{x}(t) = A_c x(t) + B_c u(t), \quad t_0 \leq t < t_0 + T, \quad (1d)$$

$$z(t) = C_c x(t) + D_c u(t), \quad t_0 \leq t < t_0 + T, \quad (1e)$$

$$\bar{z}(t) = \bar{z}_k, \quad t_k \leq t < t_{k+1}, \quad k \in \mathcal{N}, \quad (1f)$$

$$\tilde{z}(t) = z(t) - \bar{z}(t), \quad t_0 \leq t < t_0 + T, \quad (1g)$$

with the stage cost function

$$l_c(\tilde{z}(t)) = \frac{1}{2} \|W_z \tilde{z}(t)\|_2^2 = \frac{1}{2} (\tilde{z}(t)' Q_c \tilde{z}(t)), \quad (2)$$

where \bar{z} is the reference and is assumed to be piecewise constant. $Q_c = W_z' W_z$ is a symmetric positive semi-definite weight matrix. $T = NT_s$ is the control horizon and $\mathcal{N} = 0, 1, \dots, N-1$.

The corresponding discrete-time (DT) equivalent of (1) is

$$\min_{x,u} \phi = \sum_{k \in \mathcal{N}} l_k(x_k, u_k) \quad (3a)$$

$$s.t. \quad x_0 = \hat{x}_0, \quad (3b)$$

$$x_{k+1} = Ax_k + Bu_k, \quad k \in \mathcal{N}, \quad (3c)$$

with the stage costs

$$l_k(x_k, u_k) = \frac{1}{2} \begin{bmatrix} x_k \\ u_k \end{bmatrix}' Q \begin{bmatrix} x_k \\ u_k \end{bmatrix} + q_k' \begin{bmatrix} x_k \\ u_k \end{bmatrix} + \rho_k, \quad k \in \mathcal{N}, \quad (4)$$

where Q is a symmetric positive semi-definite matrix and

$$Q = \begin{bmatrix} Q_{xx} & Q_{xu} \\ Q_{ux} & Q_{uu} \end{bmatrix}, \quad q_k = M \bar{z}_k, \quad \rho_k = l_c(\bar{z}_k) T_s. \quad (5)$$

LQ-OCPs are fundamental in optimal control theory due to their simplicity and mathematical tractability (Frison and Jørgensen, 2013; Jørgensen et al., 2012). They play a central role in optimal control theory, analogous to the role of quadratic programs (QPs) in optimization theory. LQ-OCPs also have a strong connection with other advanced control algorithms, such as model predictive control (MPC). This relationship arises from using LQ-OCPs as the optimization problem within the LMPC framework. In this paper, we extend the LQ-OCP (1) to CT time-delay systems and apply exact numerical discretization to obtain the DT equivalent for numerical optimization (3). The exact discretization of CT LQ-OCPs with time delays was first introduced by Zhang et al. (2024a,b). We demonstrate its application in process-industry-relevant model predictive controllers for time-delay processes. The system dynamics are described using a multi-input, multi-output (MIMO) CT stochastic transfer function representation

$$\mathbf{Z}(s) = G(s)U(s) + H(s)\mathbf{W}(s), \quad (6a)$$

$$\mathbf{Y}(s) = \mathbf{Z}(s) + \mathbf{V}(s), \quad (6b)$$

and the transfer function matrices, $G(s)$ and $H(s)$, for the deterministic and stochastic systems are

$$G(s) = \begin{bmatrix} g_{11}(s) & \cdots & g_{1n_u}(s) \\ \vdots & \ddots & \vdots \\ g_{n_z1}(s) & \cdots & g_{n_z n_u}(s) \end{bmatrix}, g_{ij}(s) = \frac{b_{ij}(s)}{a_{ij}(s)} e^{-\tau_{ij}s}, \quad (7a)$$

$$H(s) = \begin{bmatrix} h_{11}(s) & \cdots & h_{1n_w}(s) \\ \vdots & \ddots & \vdots \\ h_{n_z1}(s) & \cdots & h_{n_z n_w}(s) \end{bmatrix}, h_{ip}(s) = \frac{d_{ip}(s)}{c_{ip}(s)}. \quad (7b)$$

The deterministic system elements $g_{ij}(s)$ are proper rational transfer functions with time delays. The stochastic system elements $h_{ip}(s)$ are strictly proper rational transfer functions without delays. $\mathbf{W}(s)$ and $\mathbf{V}(s)$ are the process and measurement noise.

The objective function is

$$\phi = \psi \left\{ \int_{t_0}^{t_0+T} l_c(\tilde{z}(t)) dt \right\}, \quad (8)$$

where ψ is some measure, i.e., in this paper the expectation, $\psi\{\cdot\} = E\{\cdot\}$, $\tilde{z}(t)$ is the tracking error (1g), and $l_c(\cdot)$ is the CT stage-cost function (2). Using the separation theorem, the resulting OCP can be realized as a Kalman filter and a certainty-equivalent linear-quadratic controller. In this paper, we use previous numerical results for the realization of such a system (Zhang et al., 2024a,b) and demonstrate how it can be used for LMPC of CT time-delay systems.

In practice, most LMPC applications employ DT LQ-OCPs with diagonal weight matrices rather than the CT formulation in (1). In the CT case, the corresponding discrete weight matrix Q is full-element, as shown in (5). Åström (1970), Åström and Wittenmark (2011), and Franklin et al. (1990) explored the discrete equivalent (1) (without time delays) and described the analytic expressions of the discrete weight matrices Q and q_k listed in (5). Pannocchia et al. (2015, 2010) proposed a novel computational procedure for the CT linear-quadratic regulator problem (CT-LQR). They noted that the discrete weight matrix Q can be computed with one exponential matrix instead of standard numerical discretization methods. The numerical experiments showed that CT-LQR offers advantages over the standard DT-LMPC. However, no results exist in the open literature on the exact numerical discretization of linear-quadratic model predictive control (with time delays) and its applications. We address this gap by presenting a description of such a model predictive controller and demonstrating its application through examples inspired by processes in the cement industry.

This paper is organized as follows. Section 2 introduces the design and discrete implementation of the CT-LMPC. Section 3 presents numerical experiments comparing the proposed CT-LMPC with the conventional DT-LMPC. Conclusions are provided in Section 3.

2. DISCRETIZATION OF MODEL PREDICTIVE CONTROL

In this section, we introduce the design and discretization of CT-LMPC.

2.1 Discretization of control model

Based on the Noise-Separation (NS) state space realization introduced by Hagdrup et al. (2016), the control model (6a) may be converted into a deterministic part $Z^d(s)=G(s)U(s)$ and a stochastic part $\mathbf{Z}^s(s)=H(s)\mathbf{W}(s)$

$$Z^d(s) \sim \begin{cases} \dot{x}_{ij}^d(t) = A_{c,ij}^d x_{ij}^d(t) + B_{c,ij}^d u_j(t - \tau_{ij}), \\ z_{ij}^d(t) = C_{c,ij}^d x_{ij}^d(t) + D_{c,ij}^d u_j(t - \tau_{ij}), \end{cases} \quad (9a)$$

$$\mathbf{Z}^s(s) \sim \begin{cases} d\mathbf{x}^s(t) = A_c^s \mathbf{x}^s(t) dt + B_c^s d\boldsymbol{\omega}(t), \\ \mathbf{z}^s(t) = C_c^s \mathbf{x}^s(t), \end{cases} \quad (9b)$$

with the system variables

$$\mathbf{x}^d = [x_{11}^d \quad x_{21}^d \quad \dots \quad x_{n_z n_u}^d]^\top, \quad z_i^d(t) = \sum_{j=1}^{n_u} z_{ij}^d(t), \quad (10a)$$

$$\mathbf{z}^d = [z_1^d \quad z_2^d \quad \dots \quad z_{n_z}^d]^\top, \quad \mathbf{z}(t) = \mathbf{z}^d(t) + \mathbf{z}^s(t), \quad (10b)$$

where we convert $Z^d(s)$ into $[i \times j]$ SISO time-delay state space models as they may have different time delays. The system state is $\mathbf{x}(t_0) = [x_0^d; \mathbf{x}_0^s]$. We define

$$\mathbf{x}^s(t_0) \sim N(\bar{x}_0^s, P_{x^s}), \quad d\boldsymbol{\omega}(t) \sim N_{iid}(0, Idt). \quad (11)$$

Let the system sampling time be T_s , such that the corresponding discrete-time systems equivalent to (9) are

$$Z^d(s) \sim \begin{cases} x_{k+1}^d = A^d x_k^d + B^d u_k, \\ z_k^d = C^d x_k^d + D^d u_k, \end{cases} \quad (12a)$$

$$\mathbf{Z}^s(s) \sim \begin{cases} \mathbf{x}_{k+1}^s = A^s \mathbf{x}_k^s + \mathbf{w}_k, \\ \mathbf{z}_k^s = C^s \mathbf{x}_k^s, \end{cases} \quad (12b)$$

and

$$\mathbf{y}_k = \mathbf{z}_k + \mathbf{v}_k, \quad \begin{bmatrix} \mathbf{w}_k \\ \mathbf{v}_k \end{bmatrix} \sim N \left(\begin{bmatrix} 0 \\ 0 \end{bmatrix}, \begin{bmatrix} R_{ww} & 0 \\ 0 & R_{vv} \end{bmatrix} \right), \quad (13)$$

where the deterministic system (12a) are obtained by stacking the all $[i \times j]$ SISO deterministic models (9a) diagonally (Zhang et al., 2024a,b).

The main advantage of using the NS state space realization is that one may apply (9b) as the model in the Kalman filter, while the controller applies (9a) as its model. Assume that the initial states x_k^d and $\hat{x}_{k|k}^s$ of the deterministic and stochastic models are available. The Kalman filter algorithm can be performed as

$$\hat{y}_{k|k-1}^s = C^s \hat{x}_{k|k-1}^s, \quad y_k^s = y_k - \hat{z}_k^d, \quad (14a)$$

$$e_k = y_k^s - \hat{y}_{k|k-1}^s, \quad \hat{x}_{k|k}^s = \hat{x}_{k|k-1}^s + K_{fx} e_k, \quad (14b)$$

with the measurement covariance and the Kalman gain

$$R_e = C^s P^s (C^s)' + R_{ww}, \quad K_{fx} = P^s (C^s)' R_e^{-1}, \quad (14c)$$

where $\hat{z}_k^d = C^d x_k^d + D^d u_k$ is the estimated deterministic output. The matrix P^s indicates the stationary stochastic state error covariance obtained by the solution of discrete-time algebraic Riccati equation (DARE)

$$P^s = A^s P^s (A^s)' - A^s P^s (C^s)' R_e^{-1} C^s P^s (A^s)' + R_{vv}. \quad (15)$$

The estimated output can be computed as

$$\hat{x}_{k+j+1|k}^s = A^s \hat{x}_{k+j|k}^s, \quad \hat{z}_{k+j|k}^s = C^s \hat{x}_{k+j|k}^s, \quad (16a)$$

$$\hat{z}_{k+j|k}^d = \hat{z}_{k+j|k}^d + \hat{z}_{k+j|k}^s, \quad j = 1, \dots, N. \quad (16b)$$

The process noise covariance R_{ww} may be computed numerically (Åström and Wittenmark, 2011; Zhang et al., 2024a,b).

2.2 Reference tracking and input regularization objectives

Define the output and input reference tracking error $\tilde{z}(t)$ as

$$\tilde{z}(t) = \begin{bmatrix} z(t) - \bar{z}(t) \\ u(t) - \bar{u}(t) \end{bmatrix} = \begin{bmatrix} z(t) - \bar{z}_k \\ u(t) - \bar{u}_k \end{bmatrix}, \quad \text{for } t_k \leq t < t_{k+1}, \quad (17)$$

where we consider piecewise constant references \bar{z} and \bar{u} . Note that the reference becomes $\bar{z}_{k+j} = \bar{z}(t) - \hat{z}_{k+j|k}^s$ for $t \in [t_{k+j}, t_{k+j+1})$ when using NS state space expressions.

We then define the following CT LQ-OCP for minimizing the output and input reference tracking error as

$$\min_{x, u, z, \tilde{z}} \phi_z + \phi_u = E \left\{ \int_{t_0}^{t_0+T} l_{c\tilde{z}}(\tilde{z}(t)) dt \right\} \quad (18a)$$

$$s.t. \quad \mathbf{x}(t_0) \sim N(\hat{x}_0, P_0), \quad (1c), \quad (9), \quad (10), \quad (17), \quad (18b)$$

with the stage cost function $l_{c\tilde{z}}(\tilde{z}(t))$

$$l_{c\tilde{z}}(\tilde{z}(t)) = \frac{1}{2} \|W_{\tilde{z}} \tilde{z}(t)\|_2^2 = \frac{1}{2} \tilde{z}(t)' Q_{c\tilde{z}} \tilde{z}(t), \quad (19)$$

where $Q_{c\tilde{z}} = \text{diag}(Q_{cz}, Q_{cu}) = W_{\tilde{z}}' W_{\tilde{z}}$. Q_{cz} and Q_{cu} are weight matrices for the reference tracking and input regularization objectives.

The corresponding DT equivalent of (18) is

$$\min_{x, u} \phi_z + \phi_u = \sum_{k \in \mathcal{N}} l_{\tilde{z}, k}(x_k, u_k) \quad (20a)$$

$$s.t. \quad x_0 = \hat{x}_0, \quad (12a), \quad (16) \quad (20b)$$

with the stage cost function $l_{\tilde{z}, k}(x_k, u_k)$

$$l_{\tilde{z}, k}(x_k, u_k) = \frac{1}{2} \begin{bmatrix} x_k \\ u_k \end{bmatrix}' Q \begin{bmatrix} x_k \\ u_k \end{bmatrix} + q'_k \begin{bmatrix} x_k \\ u_k \end{bmatrix} + \rho_k, \quad (21)$$

where

$$q_k = M[\bar{z}_k; \bar{u}_k], \quad \rho_k = l_{c\tilde{z}}([\bar{z}_k; \bar{u}_k])T_s, \quad k \in \mathcal{N}. \quad (22)$$

The DT system matrices (A, B, Q, M) may be described as a system of differential equations

$$\dot{A}(t) = A_c A(t), \quad A(0) = I, \quad (23a)$$

$$\dot{B}(t) = A(t)B_c, \quad B(0) = 0, \quad (23b)$$

$$\dot{Q}(t) = \Gamma(t)' Q_{c\tilde{z}} \Gamma(t), \quad Q(0) = 0, \quad (23c)$$

$$\dot{M}(t) = -\Gamma(t)' Q_{c\tilde{z}}, \quad M(0) = 0, \quad (23d)$$

where

$$\Gamma(t) = \begin{bmatrix} C_c & D_c \\ 0 & I \end{bmatrix} \begin{bmatrix} A(t) & B(t) \\ 0 & I \end{bmatrix}, \quad (24)$$

and $A = A(T_s)$, $B = B(T_s)$, $Q = Q(T_s)$, and $M = M(T_s)$ can be solved numerically (Zhang et al., 2024a,b).

Note that $u = [u_0; u_1; \dots; u_{N-1}]$ and $u_k = I_k u$ for $I_k = [0 \dots I \dots 0]$ and $k \in \mathcal{N}$. The system state x_k can be expressed as

$$x_k = b_k + \Gamma_k u, \quad b_k = A^k x_0, \quad \Gamma_k = \sum_{i=0}^k A^{k-1-i} B I_i. \quad (25)$$

We then rewrite the LQ-OCP (20) in the form of a QP

$$\phi_z + \phi_u = \frac{1}{2} u' H_{\tilde{z}} u + g'_{\tilde{z}} u, \quad (26)$$

where

$$H_{\tilde{z}} = \sum_{k=0}^{N-1} \begin{bmatrix} \Gamma_k \\ I_k \end{bmatrix}' Q \begin{bmatrix} \Gamma_k \\ I_k \end{bmatrix}, \quad g_{\tilde{z}} = \sum_{k=0}^{N-1} \begin{bmatrix} \Gamma_k \\ I_k \end{bmatrix}' \left(Q \begin{bmatrix} b_k \\ 0 \end{bmatrix} + q_k \right). \quad (27)$$

2.3 Input ROM and economics objectives

We then consider the LQ-OCP for penalizing the input rate-of-movement (ROM) and economic input cost

$$\phi_{\Delta u} + \phi_{eco} = \int_{t_0}^{t_0+T} l_{c\tilde{u}}(\dot{u}(t), u(t)) dt, \quad (28)$$

and the stage cost function is

$$l_{c\tilde{u}}(\dot{u}(t), u(t)) = \frac{1}{2} \|W_{c\Delta u} \dot{u}(t)\|_2^2 + q'_{ceco} u(t), \quad (29)$$

where $Q_{c\Delta u} = W'_{c\Delta u} W_{c\Delta u}$ and q_{ceco} are the weight matrices of the input ROM and the economics objectives.

Hagdrup (2019) described the discretization schemes on the input ROM penalty function using piecewise affine functions (FOH) and zero-order hold (ZOH) discretization. In this case, the discrete approximation of the input ROM penalty with ZOH discretization is

$$\begin{aligned} \phi_{\Delta u} &= \frac{1}{2} \int_{t_0}^{t_0+T} \|\dot{u}(t)\|_{Q_{c\Delta u}}^2 dt \\ &= \frac{1}{2T_s} \sum_{k \in \mathcal{N}} \|u_k - u_{k-1}\|_{Q_{c\Delta u}}^2. \end{aligned} \quad (30)$$

We perform the discretization of (28) as

$$\phi_{\Delta u} + \phi_{eco} = \sum_{k \in \mathcal{N}} l_{\tilde{u}, k}(u_k, u_{k-1}), \quad (31)$$

with the stage cost function

$$l_{\tilde{u}, k}(u_k, u_{k-1}) = \frac{1}{2} \begin{bmatrix} u_k \\ u_{k-1} \end{bmatrix}' \bar{Q}_{\Delta u} \begin{bmatrix} u_k \\ u_{k-1} \end{bmatrix} + q'_{eco} u_k, \quad (32)$$

where

$$\bar{Q}_{\Delta u} = \begin{bmatrix} Q_{\Delta u} & -Q_{\Delta u} \\ -Q_{\Delta u} & Q_{\Delta u} \end{bmatrix}, \quad Q_{\Delta u} = \frac{Q_{c\Delta u}}{T_s}, \quad q_{eco} = q_{ceco} T_s. \quad (33)$$

Consequently, along with input box and input ROM constraints, the QP expressions of the input ROM and economics objective are

$$\min_u \phi_{\Delta u} + \phi_u = \frac{1}{2} u' H_{\tilde{u}} u + g'_{\tilde{u}} u \quad (34a)$$

$$s.t. \quad u_{\min, k} \leq u_k \leq u_{\max, k}, \quad k \in \mathcal{N}, \quad (34b)$$

$$\Delta u_{\min, k} \leq \Delta u_k \leq \Delta u_{\max, k}, \quad k \in \mathcal{N}, \quad (34c)$$

where the quadratic and linear term coefficients

$$H_{\tilde{u}} = \sum_{k=1}^{N-1} \begin{bmatrix} I_k \\ I_{k-1} \end{bmatrix}' \bar{Q}_{\Delta u} \begin{bmatrix} I_k \\ I_{k-1} \end{bmatrix} + I'_0 Q_{\Delta u} I_0, \quad (35a)$$

$$g_{\tilde{u}} = \sum_{k=0}^{N-1} -I'_0 Q_{\Delta u} u_{-1} + I'_k q_{eco}. \quad (35b)$$

2.4 Soft output constraint penalty

We then introduce the soft output constraints

$$z_{k+j|k} \geq z_{\min, k+j|k} - \xi_{k+j}, \quad k = 1, 2, \dots, N, \quad (36a)$$

$$z_{k+j|k} \leq z_{\max, k+j|k} + \eta_{k+j}, \quad k = 1, 2, \dots, N, \quad (36b)$$

$$\xi_{k+j} \geq 0, \quad k = 1, 2, \dots, N, \quad (36c)$$

$$\eta_{k+j} \geq 0, \quad k = 1, 2, \dots, N, \quad (36d)$$

where ξ and η are slack variables. The output z_k is subject to the deterministic system (12). $z_{\min, k+j|k} = z_{\min, k+j} - \hat{z}_{k+j|k}^s$ and $z_{\max, k+j|k} = z_{\max, k+j} - \hat{z}_{k+j|k}^s$ are modified soft constraints.

The corresponding penalty function

$$\phi_\xi + \phi_\eta = \int_{t_0}^{t_0+T} l_{c\xi}(\xi(t)) + l_{c\eta}(\eta(t)) dt, \quad (37)$$

with the stage cost functions

$$l_{c\xi}(\xi(t)) = \frac{1}{2} \|W_{c\xi}\xi(t)\|_2^2 + q'_{c\xi}\xi(t), \quad (38)$$

$$l_{c\eta}(\eta(t)) = \frac{1}{2} \|W_{c\eta}\eta(t)\|_2^2 + q'_{c\eta}\eta(t), \quad (39)$$

where $Q_{c\xi} = W'_{c\xi}W_{c\xi}$, $Q_{c\eta} = W'_{c\eta}W_{c\eta}$, $q_{c\xi}$ and $q_{c\eta}$ are weight matrices.

We assume piecewise constant $\xi(t) = \xi_k$ and $\eta(t) = \eta_k$ for $t \in [t_k, t_k + T_s)$. The corresponding discrete equivalent is

$$\phi_\xi + \phi_\eta = \sum_{k=1}^N \frac{1}{2} (\|\xi_k\|_{Q_\xi}^2 + \|\eta_k\|_{Q_\eta}^2) + q'_\xi \xi_k + q'_\eta \eta_k, \quad (40)$$

where $Q_\xi = T_s Q_{c\xi}$, $q_\xi = T_s q_{c\xi}$, $Q_\eta = T_s Q_{c\eta}$ and $q_\eta = T_s q_{c\eta}$.

The DT penalty functions (40) can be rewritten as

$$\phi_\xi + \phi_\eta = \frac{1}{2} \begin{bmatrix} \xi \\ \eta \end{bmatrix}' H_{\bar{s}} \begin{bmatrix} \xi \\ \eta \end{bmatrix} + g'_{\bar{s}} \begin{bmatrix} \xi \\ \eta \end{bmatrix}, \quad (41a)$$

where $\xi = [\xi_1; \xi_2; \dots; \xi_N]$ and $\eta = [\eta_1; \eta_2; \dots; \eta_N]$ and

$$H_\xi = \text{diag}(Q_\xi; Q_\xi; \dots; Q_\xi), \quad g_\xi = [q_\xi \ q_\xi \ \dots \ q_\xi]', \quad (42a)$$

$$H_\eta = \text{diag}(Q_\eta; Q_\eta; \dots; Q_\eta), \quad g_\eta = [q_\eta \ q_\eta \ \dots \ q_\eta]', \quad (42b)$$

$$H_{\bar{s}} = \text{diag}(H_\xi; H_\eta), \quad g_{\bar{s}} = [g_\xi \ g_\eta]'. \quad (42c)$$

2.5 Design and implementation of CT-LMPC

Combining the objective functions and constraints introduced previously, we have

$$\min_{\{u, \xi, \eta\}} \phi = \phi_z + \phi_u + \phi_{\Delta u} + \phi_{eco} + \phi_\xi + \phi_\eta \quad (43a)$$

$$s.t. \quad x_0 = \hat{x}_0, \quad (12a), \quad (16), \quad (34b), \quad (34c), \quad (36), \quad (43b)$$

where the objective functions ϕ_z , ϕ_u , $\phi_{\Delta u}$, ϕ_{eco} , ϕ_ξ and ϕ_η are the corresponding discrete equivalent of their original CT problems.

The cost function ϕ can be expressed in the form of QP as

$$\phi = \frac{1}{2} \begin{bmatrix} u \\ \xi \\ \eta \end{bmatrix}' H \begin{bmatrix} u \\ \xi \\ \eta \end{bmatrix} + g' \begin{bmatrix} u \\ \xi \\ \eta \end{bmatrix}, \quad (44)$$

where

$$H = \begin{bmatrix} H_{\bar{z}} + H_{\bar{u}} & 0 \\ 0 & H_{\bar{s}} \end{bmatrix}, \quad g = \begin{bmatrix} g_{\bar{z}} + g_{\bar{u}} \\ g_{\bar{s}} \end{bmatrix}. \quad (45)$$

Consequently, we obtain the objective function (43) that is the discrete-time equivalent of the CT LQ-OCs introduced in previous subsections.

3. NUMERICAL EXPERIMENTS

This section presents numerical experiments with the following simulation model

$$\mathbf{Z}(s) = G(s)U(s) + G_d(s)(D(s) + \mathbf{W}(s)), \quad (46a)$$

$$\mathbf{Y}(s) = \mathbf{Z}(s) + \mathbf{V}(s), \quad (46b)$$

where $G_d(s)$ is the transfer function for the disturbance, $D(s)$, and the process noise, $\mathbf{W}(s)$.

The transfer function model can be discretized as

$$\mathbf{x}_{k+1} = A\mathbf{x}_k + B\mathbf{u}_k + E\mathbf{d}_k + G\mathbf{w}_k, \quad \mathbf{w}_k \sim N(0, R_{ww}), \quad (47a)$$

$$\mathbf{y}_k = C\mathbf{x}_k + D\mathbf{u}_k + \mathbf{v}_k, \quad \mathbf{v}_k \sim N_{iid}(0, R_{vv}). \quad (47b)$$

We develop DT-LMPC based on previous work by Hagnrup et al. (2016). The control relevant transfer function model (6) may be obtained by step response modeling or prediction-error-methods for continuous-time systems (Jørgensen and Jørgensen, 2007a,b; Olesen et al., 2013).

3.1 Closed-loop simulation - a SISO example

We perform a series of deterministic closed-loop simulations for a SISO system with the transfer functions

$$g(s) = \frac{10.12(-3.41s + 1)e^{-2.5s}}{(15.9s + 1)(24.2s + 1)}, \quad (48a)$$

$$g_d(s) = \frac{-0.5}{(5.8s + 1)(4.7s + 1)}. \quad (48b)$$

The above model is converted into state spaces (47) with $T_s = 1$ [s]. The disturbance $d_k = 2.0$ for $5 \leq t \leq 15$ [min].

The estimated control model (6) for the MPC is

$$\hat{g}(s) = \frac{10.12(-3.58s + 1)e^{-2.5s}}{(18.9s + 1)(22.2s + 1)}, \quad \hat{h}(s) = \frac{1}{s} \frac{0.6}{(s + 1)}, \quad (49)$$

where we select $\hat{h}(s)$ as an integrator to ensure the offset-free control of the controller (Muske and Badgwell, 2002; Pannocchia and Rawlings, 2003). In the SISO example, we consider ϕ_z and $\phi_{\Delta u}$ two objectives for both CT- and DT-LMPC using the same tuning parameters. For DT-LMPC, ϕ_z and $\phi_{\Delta u}$ are defined as

$$\phi = \sum_{k=0}^{N-1} \|z_{k+1} - \bar{z}_{k+1}\|_{Q_{cz}}^2 + \|u_k - u_{k-1}\|_{Q_{c\Delta u}}^2. \quad (50)$$

The prediction and control horizon is set to $N = 20$. The weight matrices are $Q_{cz} = 20$ and $Q_{c\Delta u} = 1$. The target is $\bar{z} = 2$ for $t \leq 10$ [min] and $\bar{z} = -2$ thereafter. The input constraints are $-1 \leq u \leq 1$.

To highlight the differences between CT- and DT-LMPC, we discretize both using different controller sampling times $T_s^c = \{5, 15, 25\}$ [s]. In Fig. 1a, the CT-LMPC (blue curve) and DT-LMPC (black curve) effectively regulate the system, allowing the output to track the target (red dashed line). Overshoots occur at $t = 5$ and 15 [min] due to an unknown disturbance, and the controllers can correct them after a few iterations. As T_s^c increases to 15 [s], no significant difference between the two MPCs can be observed, except for additional overshoots appear at 1 and 10 [min], as shown in Fig. 1b. In Fig. 1c, both controllers exhibit a significant decline in closed-loop performance compared to the previous cases. Increased oscillations hinder their reference tracking ability. However, CT-LMPC outperforms DT-LMPC, as its output oscillations have a smaller amplitude. While CT-LMPC stabilizes the system after 2-3 iterations, DT-LMPC fails to do so.

The simulation results of the SISO example indicate that a large sampling time can degrade the closed-loop performance of the predictive controller and may even lead to system instability. For the same system parameters,

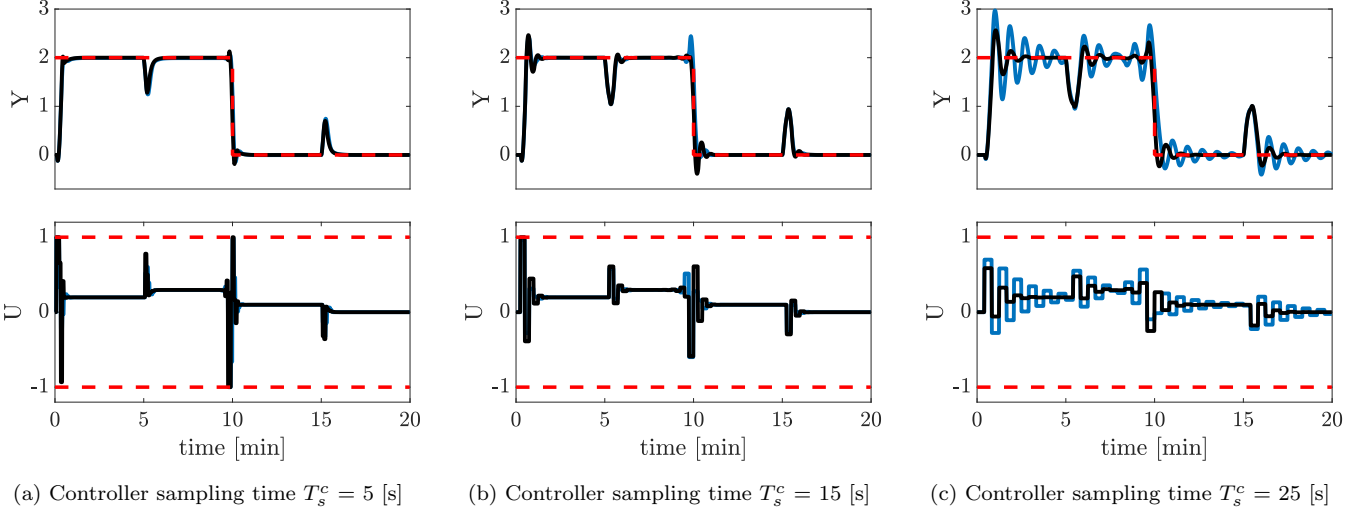


Fig. 1. SISO example deterministic closed-loop simulations with different controller sampling times $T_s^c = \{5, 15, 25\}$ [s]. The blue curves indicate the results obtained from DT-LMPC and the black curves are the results of CT-LMPC.

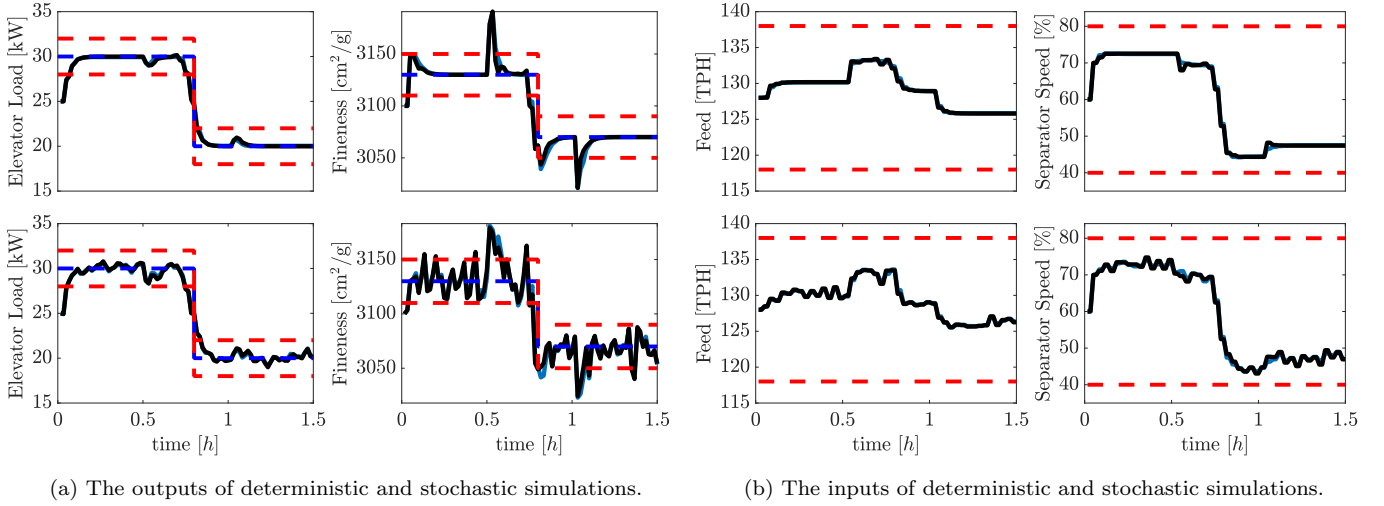


Fig. 2. Closed-loop simulations of a simulated cement mill system with the CT- and DT-LMPC.

the proposed CT-LMPC outperforms the traditional DT-LMPC, with the performance gap widening as the sampling time increases.

3.2 Closed loop simulation - a MIMO example

The MIMO example concerns the cement mill system introduced by Prasath et al. (2010) and also described in Olesen et al. (2013). The simulation model (46) has the following transfer functions

$$G(s) = \begin{bmatrix} \frac{0.62e^{-5s}}{(45s+1)(8s+1)} & \frac{0.29(8s+1)e^{-1.5s}}{(2s+1)(38s+1)} \\ \frac{-15e^{-5s}}{60s+1} & \frac{5e^{-0.1s}}{(14s+1)(s+1)} \end{bmatrix}, \quad (51a)$$

$$G_d(s) = \begin{bmatrix} \frac{-1.0e^{-3s}}{(32s+1)(21s+1)} \\ \frac{60}{(30s+1)(20s+1)} \end{bmatrix}. \quad (51b)$$

The system inputs $u = [\text{feed flow rate (TPH); separator speed (\%)}]$ and the system outputs $z = [\text{elevator load (kW); fineness (cm}^2/\text{g)}]$. The system disturbance D rep-

resents the clinker hardness (HGI). To simulate a real-world scenario, we introduce plant-model mismatch in the control model (6). The transfer functions are selected as

$$\hat{G}(s) = \begin{bmatrix} \frac{0.8e^{-5s}}{(30s+1)(15s+1)} & \frac{0.45e^{-2s}}{30.0s+1} \\ \frac{-17.7e^{-5s}}{(65s+1)(15s+1)} & \frac{9.4e^{-0.3s}}{15s+1} \end{bmatrix}, \quad (52a)$$

$$\hat{H}(s) = \text{diag} \left(\left[\frac{1}{s} \quad \frac{0.5}{s+1}; \frac{1}{s} \quad \frac{1}{s+1} \right] \right). \quad (52b)$$

The system model (46) is discretized with the sampling time $T_s = 1$ [min]. The covariances are selected as $R_{ww} = 1.0$ and $R_{vv} = \text{diag}([0.1; 50])$. The disturbance $d_k = 8$ for $0.5 \leq t \leq 1$ [h] and $d_k = 0$ otherwise.

For both CT- and DT-LMPC, the controller sampling time is $T_s^c = 2$ [min], the prediction and control horizon is $N = 60$. The weight matrices for the reference tracking, input ROM, economics and soft output constraints penalty are $Q_{cz} = \text{diag}(200, 10)$, $Q_{c\Delta u} = \text{diag}(20, 10)$, $q_{ceco} = [2; 1]$, $Q_{c\xi} = Q_{c\eta} = \text{diag}(2000, 100)$ and $q_{c\xi} = q_{c\eta} = [20; 1]$, respectively. The input hard constraints are $u_{\min} =$

$[-10; -20]$, $u_{\max} = [10; 20]$, $\Delta u_{\min} = [-5; -10]$ and $\Delta u_{\max} = [5; 10]$. The soft output constraints are given as deviation variables, $z_{\min} = [-2; -20]$ and $z_{\max} = [2; 20]$.

Fig. 2 illustrates the deterministic and stochastic closed-loop simulations of a simulated cement mill system with CT- and DT-LMPC. Both the CT-LMPC (black curves) and the DT-LMPC (blue curves) can effectively regulate the outputs towards the desired targets (blue dashed lines), while maintaining the outputs within given bounds for most of the time. At the beginning of the simulation, the outputs are outside the bounds due to initial states and the plant-model mismatch. However, this problem is corrected by both controllers after a few iterations. At $t = 0.5$ and 1.5 hours, overshoots occur due to the unknown disturbance, which both CT- and DT-LMPC can reject successfully. Additionally, a step change on the output targets at $t = 0.75$ h induces an overshoot in Fineness, with DT-LMPC exhibiting a slightly larger deviation than CT-LMPC.

The MIMO closed-loop simulations indicate that CT-LMPC and DT-LMPC achieve similar performance and converge to identical optimal solutions when appropriate sampling times and tuning parameters are used. This outcome is consistent with the SISO example in Fig. 1a. However, the CT-LMPC is easier to tune.

4. CONCLUSIONS

This paper presents the design, discretization, and implementation of CT-LMPC. We introduce various objective functions for CT-LMPC and describe how these are discretized and implemented. Numerical experiments highlight the following key observations:

1. With a small sampling time and identical (or well tuned) weight matrices, the proposed CT-LMPC and the DT-LMPC achieve similar control performance. In the limit when the sampling approaches zero, they converge to an identical optimal solution.
2. When the controller sampling time is large, the CT-LMPC performs better than the DT-LMPC. This performance gap increases as the sampling time grows.
3. It is significantly easier to tune the CT-LMPC than to tune the DT-LMPC.

Moreover, compared to conventional DT-LMPC, designing a continuous-time LQ-OCP for MPC and then discretizing it is a more natural and theoretically consistent approach. Most Nonlinear Model Predictive Controllers (NMPCs) are also designed using integrals (continuous-time) in the objective function rather than sums.

REFERENCES

- Åström, K.J. (1970). *Introduction to stochastic control theory*. Academic Press New York.
- Åström, K.J. and Wittenmark, B. (2011). *Computer-Controlled Systems: Theory and Design, Third Edition*. Dover Books on Electrical Engineering. Dover Publications.
- Franklin, G.F., Powell, J.D., and Workman, M.L. (1990). *Digital Control of Dynamic Systems*. Electrical and Computer Engineering; Control Engineering. Addison-Wesley, Reading Massachusetts, second edition.
- Frison, G. and Jørgensen, J.B. (2013). Efficient implementation of the riccati recursion for solving linear-quadratic control problems. In *2013 IEEE International Conference on Control Applications (CCA)*, 1117–1122.
- Hagdrup, M. (2019). *Model predictive control for systems described by stochastic differential equations*. Ph.D. thesis, Technical University of Denmark, Kgs. Lyngby, Denmark.
- Hagdrup, M., Boiroux, D., Mahmoudi, Z., Madsen, H., Kjølstad Poulsen, N., Poulsen, B., and Jørgensen, J.B. (2016). On the significance of the noise model for the performance of a linear MPC in closed-loop operation. *IFAC-PapersOnLine*, 49(7), 171–176. 11th IFAC Symposium on Dynamics and Control of Process Systems Including Biosystems DYCOPS-CAB 2016.
- Jørgensen, J.B., Frison, G., Gade-Nielsen, N.F., and Damman, B. (2012). Numerical methods for solution of the extended linear quadratic control problem. *IFAC Proceedings Volumes*, 45(17), 187–193. 4th IFAC Conference on Nonlinear Model Predictive Control.
- Jørgensen, J.B. and Jørgensen, S.B. (2007a). Comparison of Prediction-Error-Modelling Criteria. In *2007 American Control Conference*, 140–146.
- Jørgensen, J.B. and Jørgensen, S.B. (2007b). MPC-Relevant Prediction-Error Identification. In *2007 American Control Conference*, 128–133.
- Muske, K.R. and Badgwell, T.A. (2002). Disturbance modeling for offset-free linear model predictive control. *Journal of Process Control*, 12(5), 617–632.
- Olesen, D.H., Huusom, J.K., and Jørgensen, J.B. (2013). A tuning procedure for ARX-based MPC of multivariate processes. In *2013 American Control Conference*, 1721–1726.
- Pannocchia, G., Rawlings, J.B., Mayne, D.Q., and Mancuso, G.M. (2015). Whither discrete time model predictive control? *IEEE Transactions on Automatic Control*, 60(1), 246–252.
- Pannocchia, G., Rawlings, J.B., Mayne, D.Q., and Marquardt, W. (2010). On computing solutions to the continuous time constrained linear quadratic regulator. *IEEE Transactions on Automatic Control*, 55(9), 2192–2198.
- Pannocchia, G. and Rawlings, J. (2003). Disturbance models for offset-free model-predictive control. *AIChE Journal*, 49, 426–437.
- Prasath, G., Recke, B., Chidambaram, M., and Jørgensen, J.B. (2010). Application of soft constrained MPC to a cement mill circuit. *IFAC Proceedings Volumes*, 43(5), 302–307. 9th IFAC Symposium on Dynamics and Control of Process Systems.
- Zhang, Z., Hørsholt, S., and Jørgensen, J.B. (2024a). Numerical discretization methods for linear quadratic control problems with time delays. In *12th IFAC Symposium on Advanced Control of Chemical Processes (ADCHEM 2024)*, volume 58, 874–880.
- Zhang, Z., Svendsen, J.L., Kaysfeld, M.W., Andersen, A.H.D., Hørsholt, S., and Jørgensen, J.B. (2024b). Numerical discretization methods for the extended linear quadratic control problem. In *2024 European Control Conference (ECC)*, 505–511.